Available online at www.sciencedirect.com

ScienceDirect

IFAC Papers Online CONFERENCE PAPER ARCHIVE

IFAC PapersOnLine 55-9 (2022) 158–163

Real-Time Data-Driven Electromechanical Oscillation Monitoring using Dynamic Mode Decomposition with Sliding Window

Orlando Delgado Fernández *. Sini Tiistola *. Azwirman Gusrialdi*

**Department of Automation Technology and Mechanical Engineering, Tampere University, Finland (e-mails: orlando.df.90@gmail.com, sini.tiistola@outlook.com, azwirman.gusrialdi@tuni.fi)*

Abstract: Due to the complexity of the power system model, model-free or data-driven methods are promising for real-time electromechanical oscillations monitoring and allow grid operators to better manage the grid security and maximize transfer capacity during real-time operation. Dynamic mode decomposition (DMD) is a promising data-driven method and has been recently applied for electromechanical oscillations monitoring. However, it is still not clear what influence the length of time-window, power system eigenvalues and the use of data from pre-, during, and post-disturbances have on the estimation accuracy of the DMD. This work aims to investigate the above issues by performing a systemic analysis on three benchmark test systems. It is shown that the ultra-low frequency mode and large disturbances can negatively affect the estimation result of DMD method. In addition, it is found that the time-window length of 10 *s* is suitable in ensuring the best estimation accuracy/performance of the DMD with a sliding window.

Keywords: Electromechanical oscillations monitoring, Dynamic Mode Decompositions, time-window length, WAMS.

1. INTRODUCTION

1.1 Motivation

Wide area measurement systems (WAMS) using data from phasor measurement units (PMU) facilitates the development of real-time security assessment tools which complement the existing SCADA/EMS systems. An example of the real-time security assessment tools is the power oscillation monitoring (related to small-signal stability) implemented in the ABB PSGuard which assists Fingrid operators (Finnish power grid) in detecting when the stability limit is exceeded and further taking corrective measures to move the state system from alert to normal state (i.e., preventing the power system to enter an emergency or extreme state). In order to realize such real-time security assessment tool, it is crucial that the data-driven method being used to run sufficiently fast, provide accurate results and capture the power system dynamics (i.e., monitoring with good performance).

Several data-driven methods used for electromechanical oscillations monitoring include Prony Analysis, Matrix Pencil, Empirical Mode Decomposition, Eigensystem Realization Algorithms (ERA), Dynamic Mode Decomposition (DMD). Among those approaches, DMD has advantages in that it allows robust estimation (against measurement noise) of the dominant eigenvalues and eigenvectors which can be used to calculate the mode shapes and participation factor and thus making operator decision-taking less complicated (M. Zuhaib et al, 2021, A. Alassaf et al, 2019). Therefore, in this work we focus on the DMD method. The application of DMD to power system is relatively new and hence there are still many open questions related to its settings and performance.

1.2 Related work on DMD application in power system

To the best of our knowledge, DMD was used for the first time in (Barocio et al, 2015) where its potential is compared with small-signal stability analysis (SSSA) using simulation data and focusing on coherency identification and mode shapes of the generators.

Following the above mentioned work, many of the related works focus on analyzing the DMD's robust, such as its estimation accuracy, under noisy measurement. For example, the authors in (A. Alassaf et al, 2019) show that DMD performs well using real noisy measurements during an unstable oscillation. New strategies to improve DMD's robustness under noisy measurements are proposed in (D. Yang et al, 2019, V. T. Priyanga et al, 2021, M. Zuhaib et al, 2021, A. Alassaf et al, 2021). On the other hand, the work (J. Ramos et al, 2019) investigates how many nodes (and their locations) are required to be monitored in order to achieve an accurate assessment on the power grid disturbances.

All the previously mentioned work analyze DMD estimation's potential and robustness for one static time-window using post-disturbance measurement and different time-window lengths as summarized in Fig. 1. However, in practice the measurements are changing over the time, e.g., during the oscillations monitoring in real-time using DMD. Hence, using the static time-window may lead to a poor evaluation in comparison to the use of sliding (moving) time-window. The authors in (S. Mohapatra et al, 2016) consider a sliding window for DMD algorithm, however similar to the previously mentioned work they only use post-disturbance data. Specifically, DMD's accuracy is evaluated for different

* The work of Orlando Delgado was supported by Finnish National Agency for Education.

10.1016/j.ifacol.2022.07.028

time-window lengths (i.e., settings) and it is suggested to use a time-window length of 7 *s* which can be modified based on the application or preference.

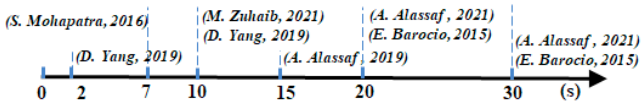

Figure 1. Time-window lengths used by the related work.

The length of time-window plays an important role in the performance of DMD algorithm for the purpose of real-time monitoring. DMD with a long time-window is computationally expensive and may affect the monitoring speed. On the other hand, DMD with a short time-window length may affect the estimation's accuracy due to measurements fluctuations (S. Mohapatra et al, 2016). To the best of our knowledge, there is still little work, in particular when utilizing a sliding window, which systematically analyze the influence of the length of time-window on the accuracy of DMD's estimation and further investigate the suitable length of the time-window. In addition, it is not totally clear about the effect of power system eigenvalues and the use of data from pre-, during, and post-disturbances on the estimation result of the DMD algorithm.

1.3. Contributions of the paper

This work aims to address the previously mentioned gaps. Specifically, the contributions of the paper are summarized as follows: i) DMD performance is tested for several case studies and the results show that DMD algorithm yields a misleading estimation when data-window has snapshots of different signals after a large disturbance; ii) It is reported for the first time that the dominant ultra-low frequency modes (f< 0,1 Hz) may negatively affect the estimation results of DMD algorithm when using small time-window lengths; iii) The analysis demonstrates that the time-window length plays a critical role in ensuring a reliable DMD performance. It is found that the window length of 10 *s* is suitable in ensuring the best DMD performance for a broad power system test systems.

The rest of the paper is organized as follows. Section 2 describes briefly the principal steps of the DMD Algorithm followed by problem statement. The case studies and the most relevant results are presented in Section 3. Finally, Section 4 concludes with the conclusions and recommendations.

2. DMD ALGORITHM AND PROBLEM FORMULATION

2.1 Review of Dynamic Mode Decomposition algorithm for electromechanical oscillations monitoring

The idea of DMD is to fit the nonlinear power system dynamics using the following linearized power system model

$$x_{k+1} = \boldsymbol{A}x_k \tag{1}$$

by computing the best-fit linear operator $\boldsymbol{A} \in \mathbb{R}^{n\times n}$ using available state measurements (data) $x_k = x(k\Delta t) \in \mathbb{R}^n$ corresponding to the power system dynamics where Δt is the sampling time of the measurements and $k = 0,1,2,\ldots$ (Burton and Kutz, 2019).

To this end, the snapshots x_k which include generators speed, rotor angle or buses voltage are sent to the energy control center (ECC) in every Δt seconds. ECC then constructs two matrices $\boldsymbol{X}_1^{m-1} \in \mathbb{R}^{n\times(m-1)}$ and $\boldsymbol{X}_2^{m} \in \mathbb{R}^{n\times(m-1)}$ using m snapshots of measurements taken during a time-window of length $T = m\Delta t$ given by

$$\boldsymbol{X}_1^{m-1} = \begin{bmatrix} | & | & & | \\ x_p & x_{p+1} & \ldots & x_{p+m-1} \\ | & | & & | \end{bmatrix}, \boldsymbol{X}_2^{m} = \begin{bmatrix} | & | & & | \\ x_{p+1} & x_{p+2} & \ldots & x_{p+m} \\ | & | & & | \end{bmatrix} \tag{2}$$

Next, using the data matrices in (2), linear approximation in (1) can be described as

$$\boldsymbol{X}_2^{m} \approx \boldsymbol{A}\boldsymbol{X}_1^{m-1} \tag{3}$$

As a result, the best-fit matrix $\boldsymbol{A}$ can be calculated as

$$\boldsymbol{A} = \boldsymbol{X}_2^{m}(\boldsymbol{X}_1^{m-1})^{\dagger} \tag{4}$$

where † denotes the pseudo-inverse. As the calculation of (pseudo) inverse of a high dimensional matrix is expensive, a Singular Value Decomposition (SVD) of the $\boldsymbol{X}_1^{m-1}$ is carried out with rank *r* resulting in the following

$$\boldsymbol{X}_1^{m-1} \approx \widetilde{\boldsymbol{U}}\widetilde{\boldsymbol{\Sigma}}\widetilde{\boldsymbol{V}}^{*} \tag{5}$$

where $\widetilde{\boldsymbol{U}} \in \mathbb{C}^{n\times r}$, $\widetilde{\boldsymbol{\Sigma}} \in \mathbb{C}^{r\times r}$, $\widetilde{\boldsymbol{V}} \in \mathbb{C}^{m\times r}$, the notation $*$ denotes the complex conjugate transpose, $r \le m$ denotes either the exact or approximate rank of the data matrix $\boldsymbol{X}_1^{m-1}$ and the matrixes satisfy $\widetilde{\boldsymbol{U}}^{*}\widetilde{\boldsymbol{U}} = \boldsymbol{I}$ and $\widetilde{\boldsymbol{V}}^{*}\widetilde{\boldsymbol{V}} = \boldsymbol{I}$. Hence, the pseudo-inverse can then be calculated as $(\boldsymbol{X}_1^{m-1})^{\dagger} = \widetilde{\boldsymbol{V}}\widetilde{\boldsymbol{\Sigma}}^{-1}\widetilde{\boldsymbol{U}}^{*}$ and substituting it into (4) yields

$$\boldsymbol{A} = \boldsymbol{X}_2^{m}\widetilde{\boldsymbol{V}}\widetilde{\boldsymbol{\Sigma}}^{-1}\widetilde{\boldsymbol{U}}^{*} \tag{6}$$

For electromechanical oscillations monitoring we are interested in estimating the r dominant eigenvalues. Hence, a reduced matrix $\widetilde{\boldsymbol{A}} \in \mathbb{R}^{r\times r}$ is calculated by projecting $\boldsymbol{A}$ onto $\widetilde{\boldsymbol{U}}$ basis such that

$$\widetilde{\boldsymbol{A}} = \widetilde{\boldsymbol{U}}^{*}\boldsymbol{A}\widetilde{\boldsymbol{U}} = \widetilde{\boldsymbol{U}}^{*}\boldsymbol{X}_2^{m}\widetilde{\boldsymbol{V}}\widetilde{\boldsymbol{\Sigma}}^{-1} \tag{7}$$

After computing the dominant dynamics in (7), the dominant eigenvalues and eigenvectors are given by

$$\widetilde{\boldsymbol{A}}\boldsymbol{W} = \boldsymbol{W}\boldsymbol{\Lambda} \tag{8}$$

where the diagonal entries of $\boldsymbol{\Lambda} \in \mathbb{C}^{r\times r}$ are the eigenvalues which also correspond to the eigenvalues of $\boldsymbol{A}$ while $\boldsymbol{W} \in \mathbb{C}^{r\times r}$ are the associated eigenvectors. Finally the relation between the eigenvalues $\bar{\lambda}_j(A)$ and the eigenvalues of the continuous-time version of dynamics (1), denoted by λ_j is given by

$$\lambda_j = \ln(\bar{\lambda}_j)/\Delta t \tag{9}$$

Where $\lambda_j = \sigma_j \pm j2\pi f_j$ and the damping ratio is $\xi_j = -\sigma_j/\sqrt{(\sigma_j)^2 + (2\pi f_j)^2}$. In the remaining sections, we are going to focus on the eigenvalues of the continuous-time dynamics.

2.2 Problem formulation

Real-time monitoring by DMD is carried out through a sliding window, that is the dominant eigenvalues are estimated using data matrices in (2) with a fixed length of window T and by taking p=0,1,2,3,… To this end, we aim at investigating the following research questions which are still not addressed in the related work: 1) How is the accuracy of DMD algorithm for real-time monitoring when the used measurement data corresponds to the pre-, during, and post-disturbances condition? 2) Could the power system's eigenvalues with ultra-low frequency affect the accuracy of DMD algorithm? 3) What is the suitable time-window length T resulting in an accurate estimation and applicable to a broad power system test systems?

3. MAIN RESULTS: CASES STUDY

To answer the research questions in the previous section, we performed numerical analysis on three benchmark systems, namely Single Machine Infinite Bus (SMIB), 2-Area, 4-generator system and Australian equivalent system by considering different disturbances for obtaining the measurements (simulation data). Note that these benchmarks have been widely used in the related work to study electromechanical oscillations.

SMIB is modeled using MATLAB while two other benchmarks are modeled using DigSILENT PowerFactory 2021. In the cases of 2-Area and Australian power systems, conventional generators are modeled by considering Automatic Voltage Regulator (AVR) and Power System Stabilizers according to IEEE Std 421.5-2016 whose settings, power system's initial conditions, SVC's AVRs, and the rest of parameters can be found in (M. Gibbard et al, 2010 and P. Kundur, 1994).

For the sake of simplicity, time delay on the communication and DMD calculation are not considered in the case studies as its value is relatively small in comparison to the time response related to electromechanical response of the power system and thus does not affect the estimation's results. Regarding the WAMS, it is assumed that PMUs are installed at all the generators whose sampling time $\Delta t = 0{,}02\ s$ similar to the units ABB RES521, SEL-451 already installed in Fingrid. Furthermore, WAMS sends the data at time step p on the speed (ω) and rotor angle (δ) of all n generators to the energy control center, that is the state in (1) at time step p equals to $x_p = [\omega_1 \dots \omega_n \quad \delta_1 \dots \delta_n]^T$. Finally, we set $r = 2n$.

3.1 Case 1: Single Machine Infinite Bus (SMIB)

In order to analyze the effect of time-window length of the sliding window on the accuracy of DMD algorithm, we consider the lengths used in the literature given by $T = (2s, 7s, 10s, 15s, 20s, 30s)$ and we use post-disturbance data to compare the estimation results. Furthermore, we use second order model for the generator and thus there is one local mode corresponding to eigenvalues $\lambda_{1,2} = -0{,}107 \pm j6{,}38$ which is excited by a small disturbance at $t = 0\ s$. Fig. 2 shows the speed and rotor angle snapshots for the duration of 40 s. Fig. 3 summarizes the estimation using DMD, including the one with T= 1 s which is equal to the mode period.

DMD with sliding window is implemented where the initial time-step for the estimation is given by $p = 0$. As can be observed from Fig. 3, the estimation of the DMD with a sliding window are $\sigma = 0{,}107\ (1/s)$ and $\omega = 6{,}384\ (rad/s)$ for all time window lengths T. Therefore, it can be concluded that for this case the length of sliding window does not have any influence on the accuracy of the DMD algorithm.

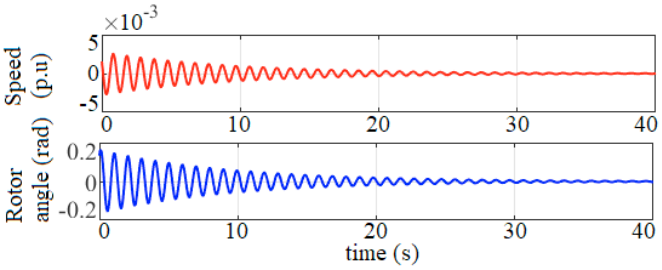

Figure 2. Speed (ω) and rotor angle (δ) variation behavior.

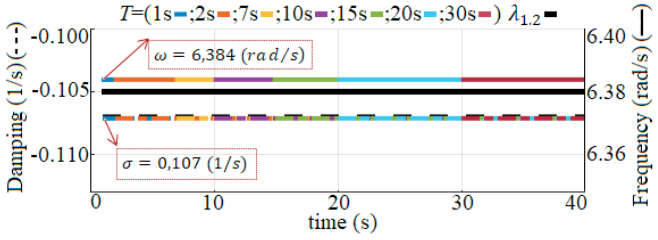

Figure 3. Damping and frequency DMD estimation of the SMIB's measurements.

Note that the analysis is carried out using post-disturbance data and one excited mode. In the following subsections, we extend the analysis by considering measurements from several PMUs, multiple dominant modes and using data obtained from pre-, during, and post-disturbances.

3.2 Case 2: Two-Area, 4-generator power system

For case 2, the linearized full state matrix $\boldsymbol{A}$ has 122 eigenvalues of which 3 modes have the worst damping ratio as shown in Table 1.

Table 1. Modes with the worst damping

Modes (λ)	f (Hz)	ξ	Generator's participation
-0,21±j3,65	0,60	0,057	G1,G2,G3,G4
-1,63±j7,03	1,12	0,22	G3,G4
-1,59±j5,86	0,93	0,26	G1,G2

Several disturbances were introduced to generate the measurements which represent normal operating conditions. First, we consider the scenario "SCE_1" where the line that connects the two areas is switched off and on at $t = 0\ s$ and $t = 24\ s$ respectively. The measurements of the four generators are shown in the Figs. 4 a and b.

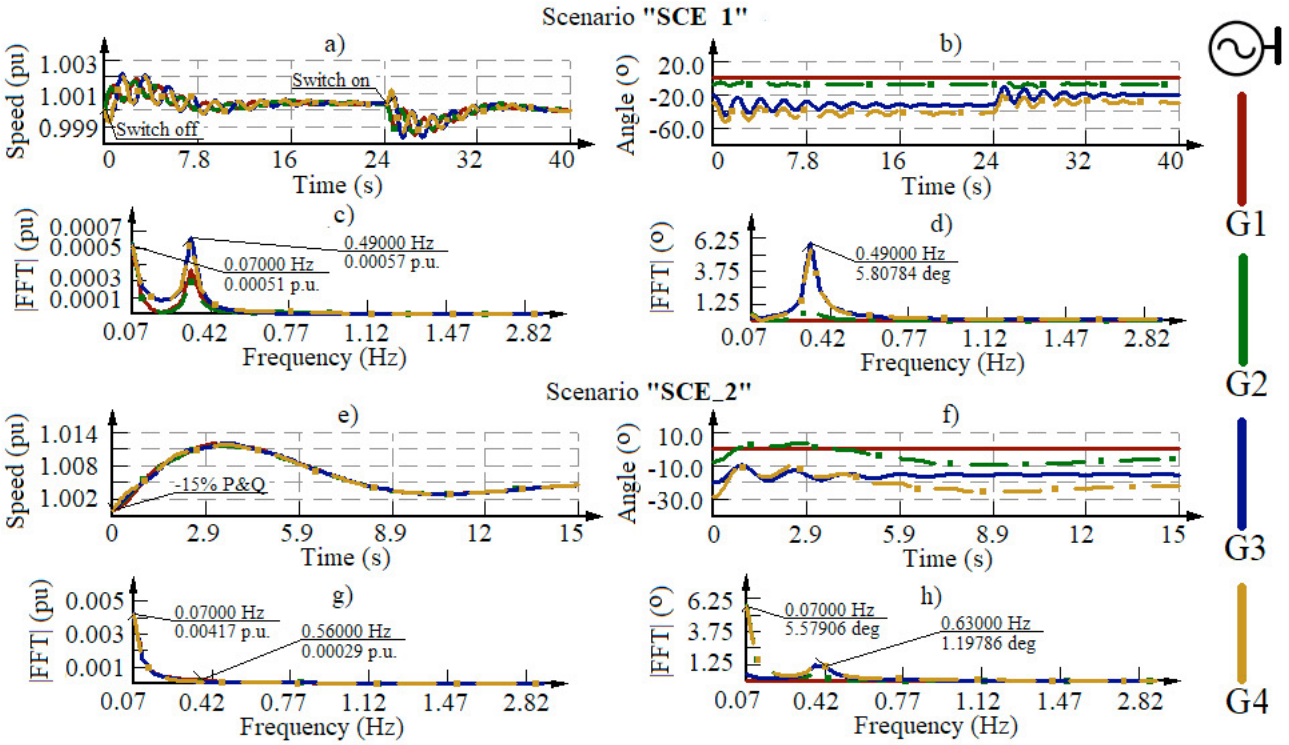

Figure 4. Behavior and Fast Fourier Transform (FFT) of the speed (a, c) and rotor angle (b, d) for the scenario "SCE_1" , behavior and FFT of the speed (e, g) and rotor angle (f, h) for the scenario "SCE_2". Fast Fourier Transform (FFT) is calculated at t=0 s to t=14,3 s .

Fast Fourier Transform (FFT) of the measurements depicted in Figs. 4 c, d shows that the local modes are not excited while both the interarea mode (0,60 Hz) and one ultra-low frequency mode (f< 0,1 Hz) corresponding to eigenvalue $\lambda = -0{,}21 \pm j0{,}44$, (0,07 Hz) are excited. Therefore, we chose this interarea mode ($\xi = 0{,}057$) in order to analyze the estimation accuracy of the DMD algorithm with a sliding window where the time-window lengths are set to $T = (1{,}66s, 2s, 7s, 10s, 15s, 20s)$. Note that the window length T= 1,66 s is also equal to the period of the interarea mode. The results are summarized in Fig. 5 which shows the damping ratio (DR) estimation of the interarea mode using DMD and the DR (dotted line) calculated via Modal Analysis (MA).

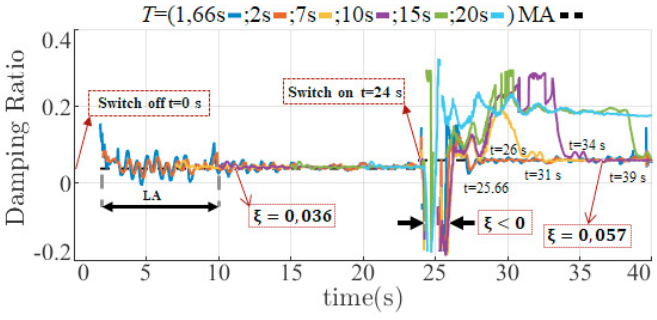

Figure 5. DR estimation of the interarea mode for "SCE_1".

It can be observed that after the second disturbance at $t = 24\ s$ the estimated damping ratio is negative ($\xi < 0$) (i.e., the power system lost its stability) which is misleading. This inaccurate estimation is because the data matrices in (2) consist of both the pre-disturbance signal and the post-disturbance signal (when the line switches on at $t = 24\ s$) and as a result the DMD algorithm performed an estimation using snapshots of two different signals. DMD algorithms started to accurately estimate the inter-area mode after one time-window length at $t = (25{,}66s, 26s, 28s, 31s, 34s, 39s)$, that is when the data matrices contain only snapshots of the post-disturbance signals. This also means that DMD algorithm requires a longer time to result in an accurate estimation for large time-window lengths $T = (15s, 20s, 30s)$ following a disturbance. This shortcoming was not reported in the previously described related work since they did not analyze the DMD algorithm with a sliding window using measurements obtained from pre, during, and post-disturbances.

In addition, it can be seen that the DR estimation has a large variation (less accurate "LA") during the first 10 seconds for the window lengths $T = (1{,}66s, 2s)$, which was not observed in case 1 for $T = (1s, 2s)$. This large variation may be related to the ultra-low frequency mode excited until $t = 14{,}3\ s$. In order to analyze in more details the influence of small time-window lengths given by $T = (1{,}66s, 2s,\ 7s, 10s)$ and the role of the ultra-low frequency mode, in the following we consider the scenario "SCE_2" when only one disturbance (15% decrease of active (P) and reactive (Q)) occurred at $t = 0\ s$ was simulated and whose measurements and FFT are shown in Figs. 4 e, f, g and h. The measurements represent higher excitation of the ultra-low frequency mode compared to interarea mode. Moreover, the estimation is performed until $t = 12\ s$ as the interarea mode excitation decreases considerably after this time. The results are summarized in Fig. 6.

First, it can be observed from Fig. 6 that the variation ("LA") of the estimation using DMD algorithm for window lengths $T = (1{,}66s, 2s)$ is larger than then the one using measurements from the scenario "SCE_1". Furthermore, the

damping ratio is incorrectly (negative value) estimated at $t = (1{,}66s, 2{,}94s, 9{,}34s)$ during the first quarter cycle of the ultra-low frequency mode. This shows that the ultra-low frequency mode affects the estimation result for window lengths $T = (1{,}66s, 2s)$.

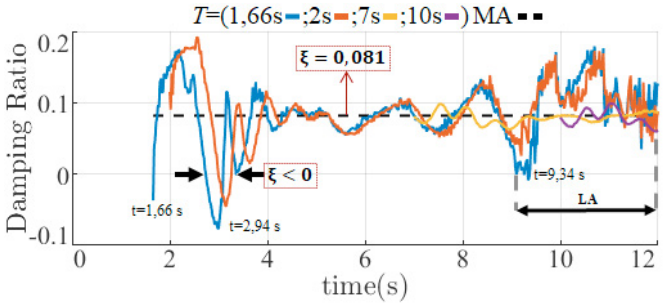

Figure 6. DR estimation of the interarea mode for "SCE_2".

The above result can also be confirmed from Fig. 7 which shows the first snapshots ($m = 83$) for window length $T = 1{,}66\ s$ with data obtained between the interval $t = 0\ s$ and $t = 1{,}66\ s$. It can be seen that as interarea mode is riding over the ultra-low frequency mode, the DMD algorithm estimates incorrect (misleading) damping ratio. This behavior of DMD algorithm was not reported in (D. Yang et al, 2019) since the ultra-low frequency mode was not excited when they considered the window of length $T = 2\ s$.

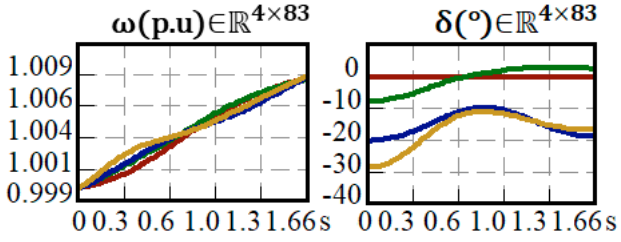

Figure 7. Snapshots that contain a data-window for a length T = 1,66 s, "SCE_2".

Note that the ultra-low frequency mode does not affect the estimation accuracy of the DMD algorithm with window lengths $T = (7s, 10s, 15s, 20\ s)$. However, using a larger window length comes at a price that the DMD algorithm takes more time to estimate the damping ratio with good accuracy since it may use mixed data from two different signals after a disturbance, as discussed previously. In the following, the lengths $T = (7s, 10s, 15s, 20\ s)$ are analyzed by considering measurements containing several excited dominants modes.

3.3 Case 3: Simplified Australian system

The simplified Australian system model has 262 eigenvalues of which 3 inter-area and 9 locals modes have the worst damping depending of the initial conditions, see Table 2.

Dominant modes are excited through two short circuits and it is assumed that protections clearing time is equal to 100 ms. The first short circuit occurs in a line between the areas 1 and 3 at $t = 0\ s$ and second fault occurs at $t = 24\ s$ between the areas 2 and 4. Figs.9 a and b show the corresponding measurements. As shown in Figs. 9 c and d, six modes (1, 2, 3, 4, 5, 6) of the worst damped modes (table 2) are excited and one mode ultra-low frequency (0,05 Hz) corresponding to $\lambda = -1{,}20 \pm j0{,}47$ is also excited. Since only the modes 4 and 5 (0,33 Hz,0,43 Hz) are excited during all the simulation time, those modes are chosen to analyze how the lengths $T = (7s, 10s, 15s, 20s)$ influences the DMD estimation.

Table 2. Modes with the worst damping of the Australian equivalent system

Modes (λ)	[f;ξ]	Modes	[f;ξ]
-0,15±j7,58$_{(1)}$	[1,21;0,02]	-0,48±j7,75$_{(7)}$	[1,23;0,06]
-0,21±j8,64$_{(2)}$	[1,37;0,02]	-0,71±j9,38$_{(8)}$	[1,49;0,08]
-0,29±j9,10$_{(3)}$	[1,44;0,03]	-0,82±j10,29$_{(9)}$	[1,63;0,08]
-0,09±j2,08$_{(4)}$	[0,33;0,04]	-0,81±j8,91$_{(10)}$	[1,41;0,09]
-0,10±j2,71$_{(5)}$	[0,43;0,03]	-0,84±j7,85$_{(11)}$	[1,25;0,10]
-0,19±j4,22$_{(6)}$	[0,67;0,04]	-0,93±j5,72$_{(12)}$	[0,91;0,16]

DMD algorithm accurately estimate the two modes for all the lengths as illustrated in Figs. 8 and 10. However, the estimation results in a big variation (less accuracy) for $T = 7s$ especially for mode 5. Notice that DMD algorithm also yields an inaccurate estimation after the second disturbance $t = 24\ s$ as the algorithm uses snapshots of two different signals, similar to the case 2. However, it can be observed that after the second disturbance, the DMD algorithm starts to estimate the correct damping ratio faster than the one in the case 2. Recall that for the case 2, DMD algorithm requires a time equal to the time-window length in order to estimate the correct values again.

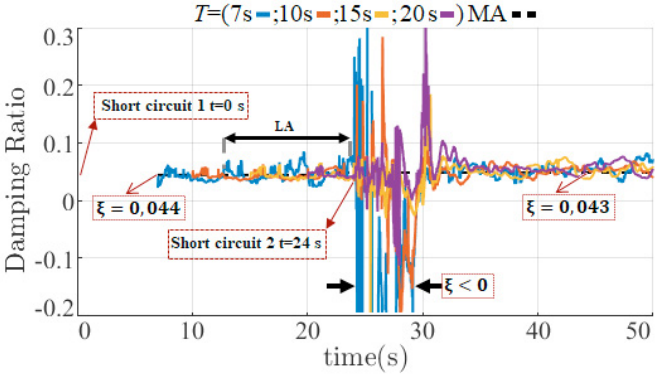

Figure 8. DR estimation of the interarea mode 4 (0,3 Hz).

To summarize, analysis of all the three cases have demonstrated that the length of sliding window plays an important role in the estimation accuracy of the DMD algorithm for real-time monitoring. In addition, it is shown from the case studies by considering the window lengths $T = (2s, 7s, 10s, 15s, 20s, 30s)$ that the length $T = 10\ s$ yields the best performance w.r.t. both estimation' accuracy and recovery time.

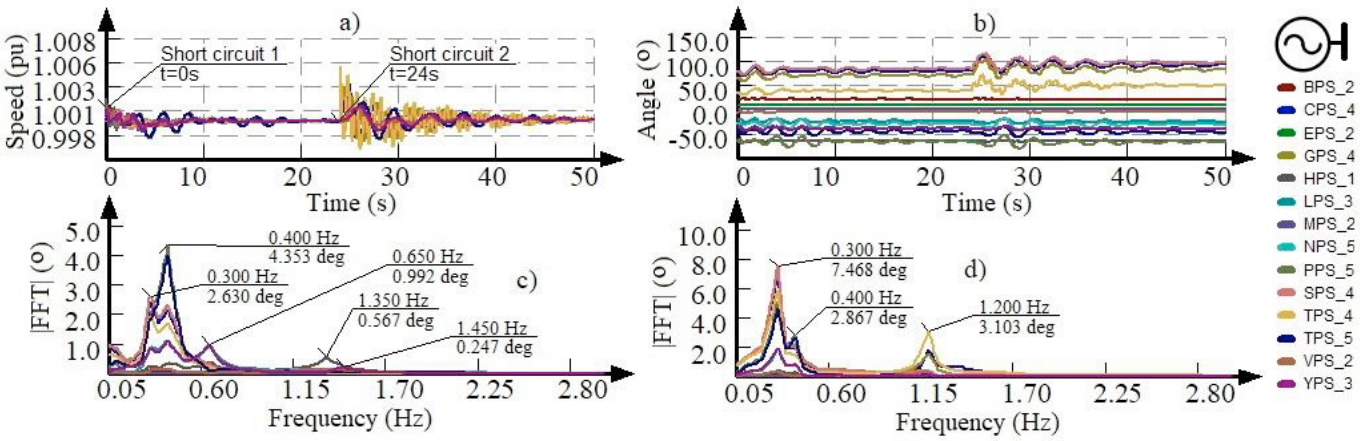

Figure 9. Behavior of the speed and rotor angle a) and b). Fast Fourier Transform (FFT) of the rotor angles at t=0 s and t=24 s, (c), d)).

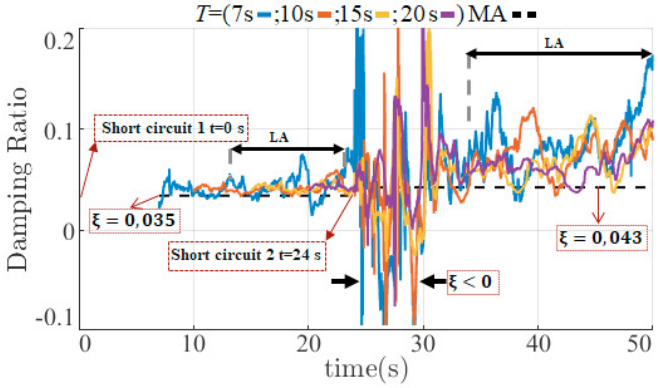

Figure 10. DR estimation of the interarea mode 5 (0,45 Hz).

3.4 Case 3: Analyzing the measurements number

4. CONCLUSIONS

Based on the analysis of the influence of the length of time-window on real-time monitoring using DMD algorithm, the following answers to the research questions are obtained: 1) the estimation of DMD algorithm can be misleading when the data-window contains snapshots of different signals after a large disturbances; 2) Ultra-low frequency mode affects the estimation result when small window length, e.g., $T = (1{,}66s, 2s)$ is used, and in the worst case yielding a negative damping ratio; 3) Based on measurements of three benchmarks and by considering different eigensystem, pre-, during, and post-disturbances conditions, it is found that the time-window of length $T = 10\ s$ ensures the best DMD performance for a broad power system test systems. As a future work, we aim to reduce the window length and improve the accuracy of DMD.

REFERENCES

A. Alassaf and L. Fan (2019). Dynamic Mode Decomposition in Various Power System Applications. *2019 North American Power Symposium (NAPS)*, page 1–6.

A. Alassaf and L. Fan (2021). Randomized Dynamic Mode Decomposition for Oscillation Modal Analysis. *IEEE Transaction on Power Systems*, volume (36), page 1399–1408.

D. Yang, T. Zhang, G. Cai, B. Wang and Z. Sun (2019). Synchrophasor-Based Dominant Electromechanical Oscillation Modes Extraction Using OpDMD Considering Measurement Noise. *IEEE Systems Journal*, volume (13), page 3185–3193.

E. Barocio, B. C. Pal, N. F. Thornhill and A. R. Messina (2015). A Dynamic Mode Decomposition Framework for Global Power System Oscillation Analysis. *IEEE Transaction on Power Systems*, volume (30), page 2902–2912.

J. Ramos and J. Kutz (2019). Dynamic Mode Decomposition and Sparse Measurements for Characterization and Monitoring of Power System Disturbances. *arXiv:1906.03544*.

M. Gibbard and D. Vowles (2010). *Simplified 14-Generator Model of the SE Australian Power System*. The University of Adelaide. Australia.

M. Zuhaib and M. Rihan (2021). Identification of Low-Frequency Oscillation Modes Using PMU Based Data-Driven Dynamic Mode Decomposition Algorithm. *IEEE Access*, volume (9), page 49434-49447.

P. Kundur. (1994). *Power System Stability and Control*. McGraw-Hill, Inc.

S. Burton and J. Kutz. (2019). *Data-Driven Science and Engineering: Machine Learning, Dynamical Systems, and Control*. Cambridge University Press.

S. Mohapatra and T. J. Overbye (2016). Fast modal identification, monitoring, and visualization for large-scale power systems using Dynamic Mode Decomposition. *2016 Power Systems Computation Conference (PSCC)*, pp. 1-7.

V. T. Priyanga, M. Chandni, N. Mohan and K. P. Soman (2019). Data-Driven Analysis for Low Frequency Oscillation Identification in Smart Grid using FB-DMD and T-DMD Methods. *2019 9th International Conference on Advances in Computing and Communication (ICACC)*, page 51–57.